

## Pre-Main Sequence Binaries with Aligned Disks?

Sebastian Wolf<sup>1</sup>, Bringfried Stecklum<sup>1</sup>, and Thomas Henning<sup>2</sup>

<sup>1</sup>*Thüringer Landessternwarte Tautenburg, Sternwarte 5, D-07778 Tautenburg, Germany*

<sup>2</sup>*Astrophysikalisches Institut und Universitäts-Sternwarte, Schillergässchen 2-3, D-07745 Jena, Germany*

**Abstract.** We present the results of a study performed with the goal to investigate whether low-mass pre-main sequence binary stars are formed by multiple fragmentation or via stellar capture. If binaries form preferentially by fragmentation, we expect their disks to be co-planar. On the other hand, the capture scenario will lead to a random distribution of disk orientations. We performed near-infrared polarization measurements of 49 young visual binary stars in the K band with SOFI at the NTT. The near-infrared excess radiation of the targets mostly point to the presence of disks. For a major fraction of the sample, evidence for disks is also obvious from other features (outflows, jets, Herbig-Haro objects). We derived the disk orientation from the orientation of the polarization vector of both components of each binary. This statistical study allows to test which hypothesis (co-planarity, random orientation) is consistent with the observed distribution of polarimetric position angles. We find evidence that the disks are preferentially aligned.

### 1. Introduction

During recent years, near-infrared (NIR) imaging and high-resolution observations yielded conclusive evidence that most (if not all) low-mass stars are born in binary and multiple stellar systems (Simon et al. 1995, Ghez et al. 1997, Leinert et al. 1997, Köhler & Leinert 1998). This finding suggests that binary formation is the rule and the birth of single stars the exception. However, the formation and survival of binary systems obviously depend upon environmental conditions (Bouvier et al. 1997). Up to now, it is not known at which stage the binary/multiple star formation mode becomes dominant. Numerical studies suggest that this occurs at early stages as the result of multiple fragmentation of molecular cloud cores (Bonnell & Bate 1994, Burkert et al. 1997, Boss 1997, Klessen et al. 1998, Bate 2000). However, other scenarios (e.g. stellar capture via close encounters, Turner et al. 1995) might lead to binary formation as well. In addition, the fragmentation process may proceed with the coalescence of the fragments.

The fact that circumstellar disks are an inevitable means to form stars implies that the individual disks surrounding the binary components represent

tracers of the binary formation mechanism. The scattering of emergent light from the star at disk surfaces and in the lobes of disk envelopes leads to a net polarization (Bastien & Ménard 1990, Whitney & Hartmann 1992, Fischer et al. 1996). The position angle of the polarization vector is indicative for the disk orientation. The formation of binaries by fission of a fragment will result in co-planar individual disks (or a circumbinary disk) because of the conservation of angular momentum. Thus, the orientation of the polarization vector for both components will be parallel. Otherwise, if binaries form by capture, the disks will have a random orientation. Another interesting scenario is the interaction of protostellar disks which would probably lead to hierarchical fragmentation where in each cascade the number of disks is approximately doubled (Watkins et al. 1998).

When addressing this question, we have to take into account that only the projection of the disk onto the tangential plane can be measured. Therefore, in the case of an individual binary, we cannot rule out that the disks have indeed different inclinations relative to the line of sight although the position angles of the polarization of two components are similar. However, a statistical study allows to test which hypothesis (co-planarity, random orientation) is consistent with the observed distribution of polarimetric position angles (see Sect. 2.3.).

First attempts to address the issue of pre-main-sequence binary polarization have been made (e.g., T Tau by Kobayashi et al. 1997, Ageorges et al. 1997, Fischer et al. 1998, Monin et al. 1998, Jensen et al. 2000). We briefly mention the results on Z CMa obtained by speckle polarimetry (Fischer et al. 1998). In this case, the K band linear polarization of the infrared primary amounts to  $P_1 = 4.2\% \pm 2.0\%$ ,  $\gamma = 173 \pm 34^\circ$  ( $\gamma$  - polarization angle) while the secondary (optical component) has  $P_1 = 8.1\% \pm 4.5\%$ ,  $\gamma = 102^\circ \pm 45^\circ$ . This investigation revealed that the spatial orientation of the individual disks is only marginally different, thus supporting the view of a common origin. Monin et al. (1998) found four sources where the rotation axes of both components are preferentially parallel but also one system where the axes are clearly not parallel. In a sample of 18 T Tauri binaries investigated by Jensen et al. (2000) in the K band, approximately 70% of the binaries have polarization angles being within  $30^\circ$  of each other.

We used the polarimetric mode of SOFI at the New Technology Telescope of ESO to test two different scenarios of binary star formation. For this purpose, a sample comprising 49 objects was selected from the binary surveys of Reipurth & Zinnecker (1993) and Ghez et al. (1997).

The near-infrared excesses of the targets mostly point to the presence of disks (e.g., Kenyon et al. 1996). For a major fraction of the sample, evidence for disks is also obvious from other features (outflows, jets, Herbig-Haro objects).

The targets have angular separations  $0.5'' \leq \rho \leq 5.3''$ . Generally, the choice of the optimum wavelength for such an investigation will represent a compromise since a large net polarization is expected at shorter wavelengths (due to the high scattering efficiency) but many of the targets are considerably reddened.

## 2. The Method

### 2.1. The General Idea

The principal method that we apply in our investigation has been firstly described by Monin et al. (1998). It is based on the assumption that PMS stars are surrounded by an optically thick disk being embedded in an optically thin dust envelope. In the general case, the light emerging from such a configuration is polarized whereby the degree of linear polarization  $P_l$  is strongly wavelength and inclination dependent and amounts to several percent in the K band. While  $P_l$  is a function of many parameters (dust density distribution in the disk, wavelength, orientation of the disk, etc.; see, e.g., Fischer et al. 1996), the polarization angle  $\gamma$  is only a function of the orientation of the disk. In the case of an optically thick disk and an optically thin circumstellar envelope, it is identical with the orientation of the long semi-axis of the ellipse which is the projection of the disk on the plane of the sky (in the case of a disk seen face-on,  $\gamma$  is not defined because the net polarization is zero). The inclination of two circumstellar disks of a PMS binary projected on the plane of the sky is therefore a function of the difference of the respective polarization angles. The influence of the projection effect is described in Sect. 2.3.

### 2.2. Polarization Mechanisms

It is now well established that the optical and near-infrared polarization of light arising from young stellar objects (YSO) is caused by light scattering on dust grains. Assuming a centro-symmetric dust density configuration around an illuminating star, the net polarization arising from scattering by spherical dust grains (see, e.g., Bastien & Ménard 1990, Whitney & Hartmann 1992, Fischer et al. 1996) or - in a more realistic scenario - by randomly oriented non-spherical grains (see Wolf et al. 2000), is equal to zero. The polarization pattern is centro-symmetric. If the star is surrounded by an optically thick disk the net polarization will have a certain value:

1. The disk partially “obscures” the optically thin shell resp. the centro-symmetric polarization pattern. The net polarization of the light arising from scattering in the shell is therefore not zero.
2. If the disk is not seen face-on, the scattering of light on the surface of the disk results in a non-centro-symmetric polarization pattern - the resulting net polarization is not zero.

The correlation between the polarization angle  $\gamma$  and the orientation of the disk is valid only under the following assumptions:

1. The disk is optically thick at the wavelength of observation. Then the assumption of the obscuration effect is fulfilled.
2. The star + disk system is embedded in an optically thin shell. The light scattering by dust grains causes the polarization of light and backscattering on the disk. The latter results in a polarization angle being parallel to the long semi-axis of the projection of the disk surface on the plane of sky.

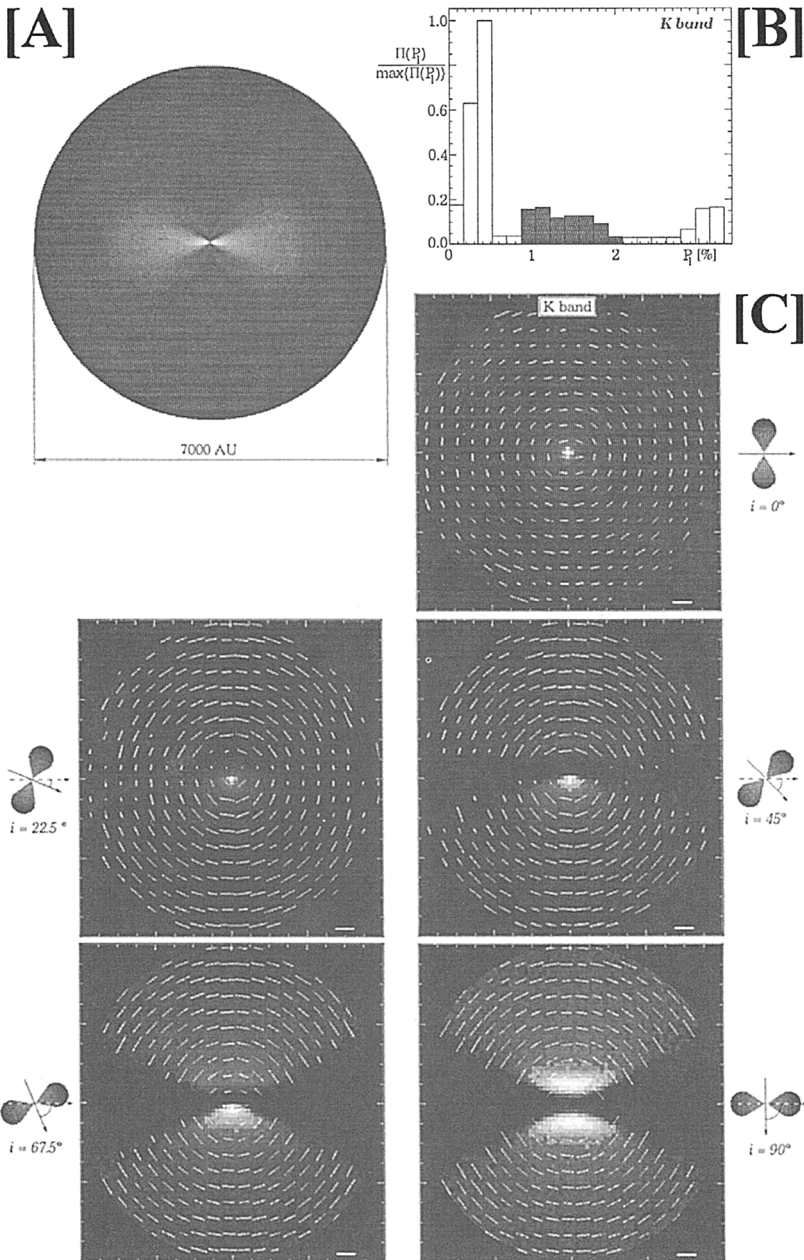


Figure 1. [A] Dust density distribution in the model of the circumstellar disk. [B] Histogram of the K band net polarization arising from the YSO configuration. [C] Intensity maps with overlaid polarization pattern of the disk for different inclinations in the K band. The polarization scale in the lower right edges of the images symbolizes a polarization degree of 100%.

Our binary sample was built using these constraints (see Sect. 3.1.).

In Fig. 1 polarization maps and the resulting probability distribution of the observable net polarization in the K band for a model of a low-mass YSO being surrounded by a circumstellar disk are shown. The spatial density structure (see Fig. 1[A]) and initial temperature distribution of the circumstellar disk ( $M = 2.3 \cdot 10^{-3} M_{\odot}$ ) results from hydrodynamical simulations performed by Yorke (1999, priv. comm.). The hydrodynamic code solves the standard equations of hydrodynamics with radiation transport and the Poisson equation for the gravitational potential (Black & Bodenheimer 1975). The two-dimensional hydrodynamic code of Różyczka (1985) with second-order accurate advection is employed. Shocks are treated by including artificial viscosity. Physical viscosity is not included and angular momentum transport during the collapse is assumed to be negligible. To derive the polarization  $P_1(i)$  of this system as a function of the inclination  $i$  perpendicular to the plane of sky, we simulated the radiative transfer (RT) with a three-dimensional continuum RT code which is based on the Monte-Carlo method (see, e.g., Wolf et al. 1999). In addition to the results from the hydrodynamical simulations, we introduce the following RT parameters: spherical dust grains consisting of “astronomical” silicates (optical data from Draine & Lee 1984, radius  $0.12 \mu\text{m}$ ); star: effective temperature  $T_{\text{eff}} = 6000 \text{ K}$ ,  $L = 2 L_{\odot}$ ; wavelength range for the simulation of the radiative transfer:  $0.03 \dots 2000 \mu\text{m}$ .

### 2.3. Inclination of Disks - Projection Effect

One has always to take into account that only the orientation of the disk resp. the orientation of its spin axis projected onto the plane of the sky can be derived from the linear polarization orientation angle  $\gamma$ . If the spin axis is rotated in the plane of the sky, the polarization angle  $\gamma$  rotates accordingly and the net polarization remains unchanged. In contrast to this, the polarization angle  $\gamma$  remains unchanged if the spin axis is rotated perpendicular to the plane of the sky. In the second case the net polarization  $P_1$  changes. Because the dust density structure of the individual disks is unknown, the inclination of a disk perpendicular to the plane of sky cannot be derived from  $P_1$ . As a consequence of this situation, the real angle between the spin axes of two disks  $\alpha$  cannot be derived with this technique. For example, a measured position angle difference  $\Delta\gamma = 0^\circ$  is not a reliable indicator for parallel spin axes (see Fig. 2).

However, this problem can be solved considering a large binary sample. If in each binary the disks are randomly oriented, the probability  $\Pi(\Delta\gamma)$  for a pair of disks to have an inclination projected on the plane of sky amounting to  $\Delta\gamma$  is constant. Even if the correct inclinations (which cannot be measured with this technique) differ from the measured inclinations in the plane of the sky, the probability distribution  $\Pi(\Delta\gamma)$  - based on measurement of the polarization angles of the binary components - is *not* modified in the case of randomly oriented disks. This comes from the fact that for every orientation of the disk in the plane of the sky (represented by the polarization angle  $\gamma$ ) the probability for the disk to be inclined by a certain angle perpendicular to the plane of the sky is constant.

In Fig. 3 the correlation between the real inclination  $\alpha$  of the disks and the position angle difference  $\Delta\gamma$  is shown for different probability distribution



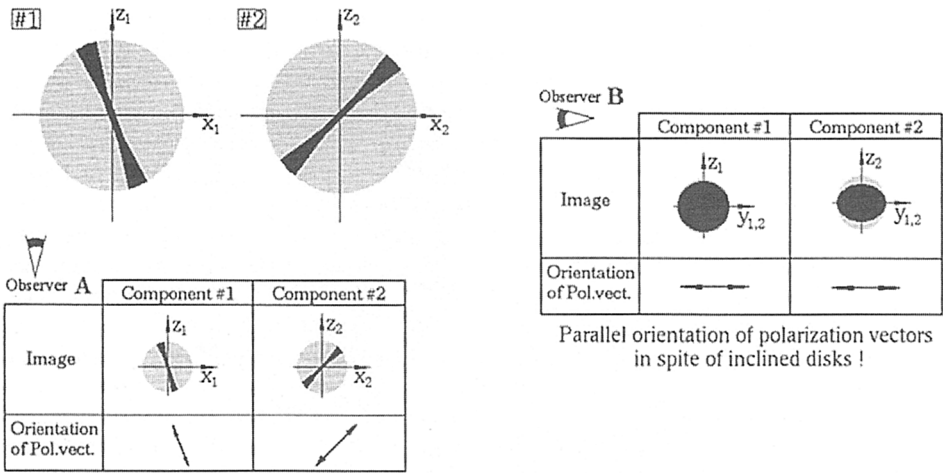


Figure 2. Explanation of the projection effect. In the upper left part of the figure two flared disks (seen edge-on, black) embedded in an optically thin circumstellar shell (grey) are shown. The y-axis of the cartesian coordinate systems  $[(x_1, y_1, z_1); (x_2, y_2, z_2)]$  is oriented perpendicular to the x-z plane pointing into the paper plane. If the plane of the sky is the  $x_1 - z_1$  (resp. the  $x_2 - z_2$ ) plane, the real inclination of the disks against each other can be measured (Observer A; see lower left table). If the  $y_1 - z_1$  (resp. the  $y_2 - z_2$ ) plane is the plane of the sky (Observer B), the polarization angle  $\gamma$  of both disks is parallel to the according y-axis. Therefore - due to the projection effect -, these disks would be assumed to be co-planar. Only on the basis of a large binary sample, a decision whether the individual disks of the binary components are in general co-planar or oriented randomly can be made (see Sect. 2.3.).

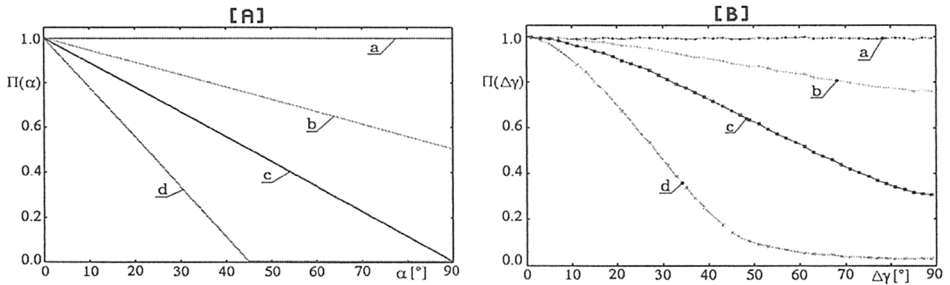


Figure 3. Correlation between [A] the distribution of the real inclinations  $\Pi(\alpha)$  of the disks and [B] the distribution of the corresponding position angle differences  $\Pi(\Delta\gamma)$  (see Sect. 2.3.). (a): perfect random orientation of the disks; (b)...(d): increasing alignment of the disks.

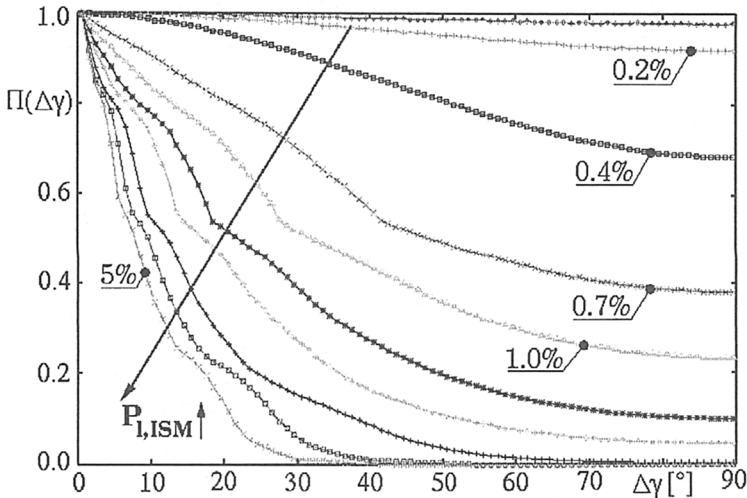


Figure 4. Probability distribution function  $\Pi(\Delta\gamma)$  for randomly oriented disks as a function of the degree of linear polarization of the ISM  $P_{1,ISM}$ . The decrease of  $\Pi(\Delta\gamma)$  steepens with increasing polarization  $P_{1,ISM}$ .  $P_{1,ISM} = 0.1, 0.2, 0.4, 0.7, 1.0, 1.5, 2.0, 3.0, 4.0,$  and  $5.0\%$ .

functions  $\Pi(\alpha)$ <sup>1</sup>. For perfectly randomly oriented disks ( $\Pi(\alpha)=\text{const.}$ ), we find  $\Pi(\Delta\gamma)=\text{const.}$ . An alignment of disks - being characterized by a decrease of the probability distribution function  $\Pi(\alpha)$  for increasing  $\alpha$  - results in a decrease of the measured distribution function  $\Pi(\Delta\gamma)$ . One has also to be aware, that even in the case of strongly - but not perfectly - aligned disks for which  $\Pi(\alpha)=0$  for  $\alpha > \alpha_0$  ( $\alpha_0 > 0$ ; see Fig. 3, distribution *d*), there is still a probability to measure position angle differences  $\Delta\gamma > \alpha_0$ .

#### 2.4. Influence of the Interstellar Polarization

As discovered by Hiltner (1949), the interaction of light of distant stars with the interstellar medium (ISM) leads to a significant linear polarization. Because this additional “polarizer” (polarization degree  $P_{1,ISM}$ , orientation angle  $\gamma_{ISM}$ ) influences the observed light of both binary components, the observed position angle difference  $\Delta\gamma$  may be reduced. Thus, even in the case of perfectly randomly oriented disks, this may lead to an apparent alignment of the disks because the probability distribution function  $\Pi(\Delta\gamma)$  would increase towards decreasing  $\Delta\gamma$ .

To estimate the influence of the interstellar polarization (ISP) on our results, we derived the K-band polarization of the model of a low-mass YSO described in Sect. 2.2.. The second step was to combine two of these disk under the assumption of random pairing ( $\Pi(\alpha)=\text{const.}$ ). Finally, the measurable apparent inclination of these disks  $\Delta\gamma$  in the plane of sky was determined taking into

<sup>1</sup>These results are based on Monte-Carlo simulations. Each distribution  $\Pi(\Delta\gamma)$  was determined based on the projection of  $10^7$  pairs of disks - following the distribution  $\Pi(\alpha)$  - onto the plane of the sky.

account the additional polarization by the ISM. Based on  $10^7$  pairs of disks, the resulting distribution function  $\Pi(\Delta\gamma)$  as a function of  $P_{1,ISM}$  is shown in Fig. 4. The decrease of the distribution  $\Pi(\Delta\gamma)$  towards increasing  $\Delta\gamma$  is strengthened by the increase of  $P_{1,ISM}$ .

### 3. Observations

#### 3.1. The Sample

As pointed out in Sect. 2.2., we have to consider PMS stars in an evolutionary stage in which they are still surrounded by an optically thick disk being embedded in an optically thin shell. The objects fulfilling these criteria are classical T Tauri stars. Therefore our sample consists of 49 close binaries (separations:  $0.5'' \dots 5.3''$ ) from the surveys of Reipurth & Zinnecker (1993), Ghez et al. (1997), and Prato & Simon (1997).

#### 3.2. The Observing Strategy

The polarization data were obtained in 1999 March 2-4 and May 28-30 at the European Southern Observatory (ESO). The images were taken using SOFI in imaging polarization mode at the New Technology Telescope (NTT). The pixel scale in this mode is  $0.292''$  per pixel.

With SOFI, polarimetry is performed by inserting in the parallel beam a Wollaston prism which splits the increasing light rays into 2 orthogonally polarized beams separated by  $48''$ . For the derivation of the Stokes vector components Q and U, the objects were observed at two different orientations of the Wollaston prism differing by 45 degrees.

To increase the signal-to-noise ratio (SNR) and for a sufficient badpixel and background subtraction we observed each object at each orientation of the Wollaston prism 5 times (offset:  $25''$ ).

### 4. Results

The histograms of the linear polarizations and the position angle differences  $\Delta\gamma$  based on 34 binaries are shown in Fig. 5. The remaining objects were excluded because the error of polarization and therefore the error of the orientation angle  $\gamma$  (for the formalism of error estimation see, e.g., Wardle & Kronberg 1974, di Serego Alighieri 1998) of at least one component of the binary system was too large ( $P_1/\sigma(P_1) < 3$ ). Thus, preferentially those binaries in which at least one component shows a very low linear polarization ( $\leq 1\%$ ), were excluded. This can also be seen in the histogram for  $P_1$  which is otherwise (for  $P_1 > 1\%$ ) in very good agreement with the simulated histogram (see Sect. 2.4., Fig. 1[B]). The distribution ( $N(\Delta\gamma)$ ) shows a strong decrease towards large angles  $\Delta\gamma$ . Assuming the ISP to cause this behaviour, the degree of linear polarization had to exceed 1% (for comparison see Fig. 4[B]). In contrast to this, the mean degree of linear polarization caused by the ISM in the K band was found to be well below 1% in average (see, e.g., Nagata 1990). Thus, the distribution  $\Pi(\Delta\gamma)$  reflects the intrinsic polarization of the binary components and therefore the alignment of their disks.



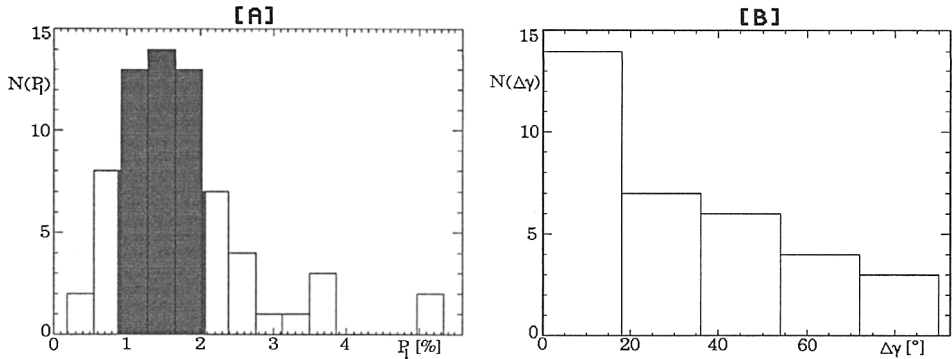


Figure 5. [A] Histogram of the polarization measured for  $2 \times 34$  binary components. The dark grey region marks the ranges in which we found a local maximum of the linear polarization in our model simulations (for comparison see Fig. 1[B]). [B] Distribution of the position angle differences  $\Delta\gamma$  of the disks in 34 binaries. For comparison see Fig. 3 and Fig. 4.

## 5. Conclusions

Based on K band observations of 49 classical T Tauri binary stars, we found intrinsic linear polarization for both components in 34 binary systems. The polarization can be explained by light scattering on spherical dust grains under the assumption of the presence of a circumstellar disk. We performed self-consistent RT simulations for a low-mass YSO surrounded by a circumstellar disk with a structure resulting from hydrodynamical simulations. The probability distribution of the polarization degree fits very well to the observed distribution derived from the polarization of all binary components.

We showed that real inclinations of the circumstellar disks in single binary systems cannot be measured using the position angle difference  $\Delta\gamma$ . But it turned out that, based on a large binary sample, one can decide if there exists an alignment mechanism. The measured probability distribution function  $\Pi(\Delta\gamma)$  shows a steep decrease towards large inclinations  $\Delta\gamma$ . Based on RT simulations we showed that this behaviour cannot be explained by the influence of the ISP.

We can therefore conclude that the disks in our sample are preferentially aligned. Thus, if stellar capture plays a role during the binary formation process, it must be followed by disk alignment processes on a timescale much smaller than the lifetime of the circumstellar disks. Otherwise, fragmentation as the basic binary formation process could explain the observed inclination distribution without any assumptions. The tail towards large inclinations can be explained by the projection effect (see Sect. 2.3.). Moreover, turbulence in the molecular cloud during the fragmentation process might lead to misaligned fragments as well (R. Klein, priv. comm.).

**Acknowledgments.** We wish to thank H.W. Yorke for providing the spatial density and temperature distribution of a protostellar disk. This research was supported by the DFG grant Ste 605/10 within the program ‘‘Physics of

star formation". It is based on observations collected at the European Southern Observatory.

## References

- Ageorges, N., Eckart, A., Monin, J.-L., Ménard, F. 1997, *A&A*, 326, 632
- Bastien, P., & Ménard, F. 1990, *ApJ*, 364, 232
- Bate, M. R. 2000, *MNRAS*, 314, 33
- Black, D. C., & Bodenheimer P. 1975, *ApJ*, 199, 619
- Bouvier, J., Rigaut F., Nadeau D. 1997, *A&A*, 323, 139
- Bonnell, I. A., & Bate, M. R. 1994, *MNRAS*, 271, 999
- Boss, A. P. 1997, *ApJ*, 483, 309
- Burkert, A., Bate, M. R., Bodenheimer, P. 1997, *MNRAS*, 289, 497
- Draine, B. T., Lee, H. M. 1984, *ApJ*, 285, 89
- Fischer, O., Henning, Th., & Yorke, H. W. 1996, *A&A*, 308, 863
- Fischer, O., Stecklum, B., & Leinert, Ch. 1998, *A&A*, 334, 969
- Ghez, A. M., McCarthy, D. W., Patience, J. L., Beck, T. L. 1997, *ApJ*, 481, 378
- Hiltner, W. A. 1949, *ApJ*, 109, 471
- Jensen, E., Donar, A. X., Mathieu, R. D. 2000, in *Birth and Evolution of Binary Stars*, ed. B. Reipurth & H. Zinnecker
- Kenyon, S. J., Yi, I., & Hartmann, L. 1996, *ApJ*, 462, 439
- Kobayashi, N., Nagata, T., Tamura, M., et al. 1997, *ApJ*, 481, 936
- Klessen, R. S., Burkert, A., Bate, M. R. 1998, *ApJL*, 510, L205
- Köhler, R., Leinert, Ch. 1998, *A&A*, 331, 977
- Leinert, Ch., Richichi, A., Haas, M. 1997, *A&A*, 318, 472
- Monin, J.-L., Ménard, F., Duchêne, G. 1998, *A&A*, 339, 113
- Nagata, T. 1990, *ApJ*, 348, L13
- Prato, L., Simon, M. 1997, *ApJ*, 474, 455
- Reipurth, B., & Zinnecker, H. 1993, *A&A*, 278, 81
- Różyczka, M. 1985, *A&A*, 143, 59
- di Serego Alighieri, S. 1998, in *Instrumentation for Large Telescopes*, ed. J. M. Rodriguez, Cambridge University Press
- Simon, M., Ghez, A. M., Leinert, Ch., et al. 1995, *ApJ*, 443, 625
- Turner, J. A., Chapman, S. J., Bhattal, A. S., et al. 1995, *MNRAS*, 277, 705
- Whitney, B. A., Hartmann, L. 1992, *ApJ*, 395, 529
- Wardle, J. F. C., Kronberg, P. P. 1974, *ApJ*, 194, 249
- Watkins, S. J., Boffin, H. M. J., Francis, N., Whitworth, A. P. 1998, *ASP*, 132, 430
- Wolf, S., Henning, Th., Stecklum, B. 1999, *A&A*, 349, 839
- Wolf, S., Voshchinnikov, N., Henning, Th. 2000, in preparation